AD-A055 205 ARMY ELECTRONICS COMMAND FORT MONMOUTH N J F/G 4/2
THE INTERNAL CLOUD RADIATION FIELD AND A TECHNIQUE FOR DETERMIN--ETC(U)
DEC 77 R D LOW

UNCLASSIFIED ECOM-5833 NL

| OF |
AD
A055205

END
DATE
FILMED
7-78
DDC

FOR FURTHER TRAN

(12)

AD

Reports Control Symbol
OSD-1366

(9) RESEARCH AND DEVELOPMENT TECHNICAL REPORT,

(14) ECOM-5833

AD A055205

AD No. ____
DDC FILE COPY

(6) # THE INTERNAL CLOUD RADIATION FIELD AND A TECHNIQUE FOR DETERMINING CLOUD BLACKNESS.

By

(10) Richard D.H. Low

(16) 1T161101A91A (17) 09

Atmospheric Sciences Laboratory

US Army Electronics Command

White Sands Missile, New Mexico 88002

(12) 28p.

(11) December 1977

DDC
RECEIVED
JUN 19 1978
A

Approved for public release; distribution unlimited.

ECOM 037620 AB

UNITED STATES ARMY ELECTRONICS COMMAND - FORT MONMOUTH, NEW JERSEY 07703

78 06 08 053

NOTICES

Disclaimers

The findings in this report are not to be construed as an official Department of the Army position, unless so designated by other authorized documents.

The citation of trade names and names of manufacturers in this report is not to be construed as official Government indorsement or approval of commercial products or services referenced herein.

Disposition

Destroy this report when it is no longer needed. Do not return it to the originator.

SECURITY CLASSIFICATION OF THIS PAGE *(When Data Entered)*

REPORT DOCUMENTATION PAGE

READ INSTRUCTIONS BEFORE COMPLETING FORM

1. REPORT NUMBER: ECOM-5833	2. GOVT ACCESSION NO.
3. RECIPIENT'S CATALOG NUMBER	
4. TITLE *(and Subtitle)*: THE INTERNAL CLOUD RADIATION FIELD AND A TECHNIQUE FOR DETERMINING CLOUD BLACKNESS	5. TYPE OF REPORT & PERIOD COVERED: R&D Technical Report
	6. PERFORMING ORG. REPORT NUMBER
7. AUTHOR(s): Richard D. H. Low	8. CONTRACT OR GRANT NUMBER(s)
9. PERFORMING ORGANIZATION NAME AND ADDRESS: Atmospheric Sciences Laboratory, White Sands Missile Range, New Mexico 88002	10. PROGRAM ELEMENT, PROJECT, TASK AREA & WORK UNIT NUMBERS: DA Task No. 1T161101A91A-09
11. CONTROLLING OFFICE NAME AND ADDRESS: US Army Electronics Command, Fort Monmouth, New Jersey 07703	12. REPORT DATE: December 1977
	13. NUMBER OF PAGES: 30
14. MONITORING AGENCY NAME & ADDRESS *(if different from Controlling Office)*	15. SECURITY CLASS. *(of this report)*: UNCLASSIFIED
	15a. DECLASSIFICATION/DOWNGRADING SCHEDULE

16. DISTRIBUTION STATEMENT *(of this Report)*

Approved for public release; distribution unlimited.

17. DISTRIBUTION STATEMENT *(of the abstract entered in Block 20, if different from Report)*

18. SUPPLEMENTARY NOTES

19. KEY WORDS *(Continue on reverse side if necessary and identify by block number)*

Blackbody	Internal radiation field
Cloud model	Cloud blackness
Upwelling radiance	Ratio test

20. ABSTRACT *(Continue on reverse side if necessary and identify by block number)*

The internal radiation fields of homogeneous and inhomogeneous stratocumulus model clouds under the same meteorological conditions were investigated at several wavelengths in the 11 μm window region. The results showed that a homogeneous cloud model may be used in place of an inhomogeneous one to deduce the upwelling radiances, but not the internal structure of the cloud radiation field. The resulting findings that in this window region the optical properties of a cloud at a shorter wavelength permit a greater penetration of the surface radiation and hence scattering by the cloud particles than those at longer wavelengths

DD FORM 1 JAN 73 1473 EDITION OF 1 NOV 65 IS OBSOLETE

78 06 08 055

SECURITY CLASSIFICATION OF THIS PAGE *(When Data Entered)*

20. ABSTRACT (cont)

lead to the development of a technique for quickly assessing the "blackness" of a cloud.

The technique requires ~~the use of~~ using two channels in the window region to establish a ratio of the observed upwelling radiances. The ratio is then compared with the reference ratio derived from a knowledge of the estimated surface temperature in what was termed the ratio test. It was shown that the estimated temperature need not be accurate. Examples are presented to demonstrate that the vertical emissivity of clouds is close to 0.95 or greater when the ratio test is satisfied. However, when the observed radiances convert to nearly the same temperature value, the cloud may be said to have an emissivity of unity and that temperature then becomes the cloud-top temperature. On the basis of this method, the temperature field generated by satellite infrared imagery may be accepted or rejected with reasonable confidence.

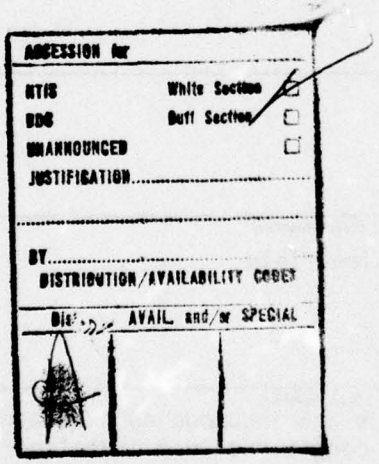

ACKNOWLEDGMENTS

The author is grateful to Dr. K. N. Liou of the University of Utah for his critical review of this paper.

TABLE OF CONTENTS

INTRODUCTION

One of the serious problems in satellite infrared imagery analyses and in the retrieval of temperature profiles in the presence of clouds from satellite soundings is how to differentiate between the derived temperature values which arise from the radiation field involving the blackbody or non-blackbody cloud. This problem has been recognized by Glahn [1] as one of several difficult problems in conjunction with the determination of cloud top heights and areal coverage. Chahine [2,3,4], among others, in a series of outstanding papers has described methods for retrieving atmospheric temperatures in the presence of clouds. However, these methods assume that the clouds are blackbodies. Although a number of papers [5,6,7,8] have examined the approximate thickness required for a cloud to radiate as a blackbody, the cloud blackness problem has not yet comprehensively been investigated. If the cloud thickness is the required parameter to determine whether a cloud temperature arises from a blackbody radiation field, then it seems that the problem is far from being satisfactorily resolved.

The purpose of this paper is to discuss the problem of the cloud blackness in the 11μm infrared window region in relation to satellite application. In examining the internal structure of the cloud radiation field, a method was developed by which the degree of the cloud blackness may be derived by adding a 10.5μm channel to, for example, the existing 12.0μm channel in the vertical temperature profile radiometer (VTPR). Consequently, it would be possible to determine the reliability of the derived temperature values. To develop the method, it is necessary to first understand physically the internal cloud radiation field. Since the primary interest was in satellite application, only the vertical upward-going radiation of clouds was investigated.

The computer program for solving the radiative transfer equation was based upon the Gauss-Seidel iteration technique [9,10] and had been checked out against published values in the literature [5,8]. For water vapor attenuation, use was made of LOWTRAN 3 [11] and the empirical formula given by Roberts et al., [12] to account for selective and continuum absorption, respectively. The computer program not only gives the cloud radiance values as a function of zenith angles at different prescribed geometric levels, but also calculates the optical properties, including the optical thicknesses and single-scattering albedos at corresponding levels.

Since an understanding of the internal structure of the cloud radiation field is essential to the development of the technique, the next section describes the cloud models to be used in the investigation. The theoretical basis then follows. In section 4, computational results are presented, and the internal radiation structures are examined. These analyses lead to the development of the technique for determining the degree of cloud "blackness" or emissivity in section 5. A few numerical examples will be given here. The final section contains the findings and conclusions.

CLOUD MODEL

Only recently have the radiative properties of clouds been studied realistically with inhomogeneous droplet and temperature distributions considered. Stephens [13], using the meteorological, microphysical, and radiation data furnished to him by Paltridge [14], investigated the inhomogeneous stratiform clouds theoretically and found the calculated downward radiances in good agreement with the observed values. Platt's observations [15] of upwelling radiances emerging at different levels from his inhomogeneous Stratocumulus Deck 2 as shown in Fig. 1 were adopted in this paper. This cloud had a thickness of about 550 m with a temperature distribution as given in his figure. From the typical humidity profile shown, it may be inferred that except for the middle region of the cloud, which was saturated, both the top and base layers were most likely subsaturated.

Platt's radiance profile in the 10.5μm window was simulated and radiance values were expressed in mW m^{-2} sr^{-1} cm, which can be readily converted to his physical unit by means of a simple formula. However, it should be noted that the choice of cloud microphysics and wavelength would in no way affect either the analysis of the internal radiation structure or the findings and conclusions.

Although no microphysics data were provided by Platt [15], on the basis of a number of cloud physics studies [16,17,18], it appears that the gamma distribution [19] with two parameters, $\alpha = 4$ and $\beta = 1$, may adequately represent the stratocumulus cloud over the ocean. The droplet sizes ranged from 0.5μm to 25μm with a mean radius of 5μm. In view of the abundant supply of sea-salt nuclei over the ocean, the upper limit of the range seems to represent a reasonable value. With the known distribution function and size range and the refractive indices for water spheres [21], Mie scattering and absorption coefficients per unit length may be calculated.

Stratocumulus Deck 2 was divided into 22 layers each 25 m thick, and radiance values were computed at each level. With the Mie coefficients known, a first approximation to the number density of droplets required to emit the desired amount of radiation at each level was made. Then the temperature profile and the estimated droplet number densities at chosen levels were fed into the computer program to generate a first estimate of upward radiances as a function of cloud depths. Adjustments were made of the number densities at several levels in each run. Platt's radiance profile was reproduced almost exactly for the 10.5μm window in four trial runs. The input meteorological and microphysical values are given in Table 1. Although the computer program is capable of accounting for water vapor attenuation both inside and outside the cloud, the attenuation of surface radiation below the cloud base was not considered since the amount of attenuation was quite small, as is evident in Fig. 1.

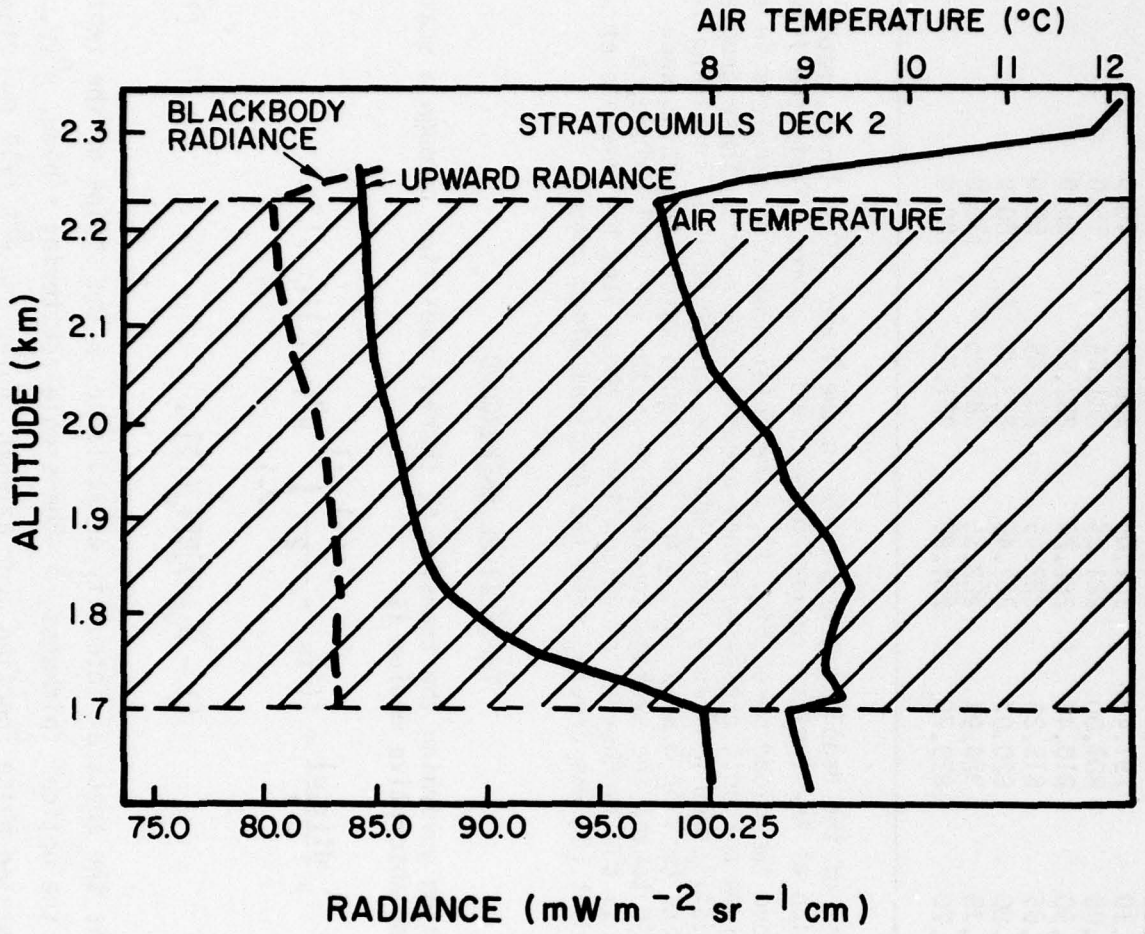

Figure 1. Profiles of vertical upward radiance, air temperature, and blackbody radiance through the stratocumulus cloud deck.

TABLE 1. INPUT METEOROLOGICAL AND MICROPHYSICAL DATA OF THE MODEL CLOUD

Height (km)	Pressure (mb)	Airtemp (°K)	Dewtemp (°K)	Droplet (cm^{-3})
2.25	777.21	280.55	279.15	5.0
2.10	791.40	281.05	280.65	10.0
2.00	801.00	281.65	281.65	15.0
1.90	810.48	282.24	282.25	25.0
1.85	815.26	282.45	282.45	50.0
1.80	820.07	282.45	282.35	100.0
1.75	824.91	282.35	282.25	130.0
1.70	829.78	281.95	281.75	120.0

Since most of the droplets concentrate in the lower 150 m layer, rapid attenuation of the surface radiation is found in approximately the first 200 m above the cloud base (Fig. 1). The total number of droplets in the 550 m column per unit cross-sectional area is 2.20×10^6. These droplets were redistributed uniformly throughout the entire column, resulting in 40 droplets cm^{-3} or 3.52×10^{-2} g m^{-3} in liquid water content at each level. By taking the average temperature in the vertical column, a homogeneous and isothermal cloud similar to those used by Yamamoto et al. [5] and Hunt [8] was created from the original cloud model.

THEORETICAL BACKGROUND

The equation governing the transfer of thermal radiation through a scattering and absorptive medium is

$$\mu \frac{dI(\tau;\mu)}{d\tau} = I(\tau;\mu) - \frac{\tilde{\omega}_o(\tau)}{2}\int_{-1}^{+1} p^o(\mu,\mu')I(\tau,\mu')d\mu'$$

$$- [1 - \tilde{\omega}_o(\tau)]B[T_c(\tau)] , \qquad (1)$$

where I is the spectral intensity or radiance, μ the cosine of the zenith angle, τ the optical thickness, $\tilde{\omega}_o$ the single-scattering albedo, $p^o(\mu,\mu')$ the integrated phase function over azimuth angle, and $B[T_c(\tau)]$ the Planck function for cloud temperature T_c at level τ. For simplicity, the wavenumber-dependent subscript has been eliminated. The above equation can be separated into two components as follows: one component denotes the external field, primarily due to surface radiation, and the other denotes the cloud emission.

For the external field (I_g),

$$\mu \frac{dI_g(\tau;\mu)}{d\tau} = I_g(\tau;\mu) - \frac{\tilde{\omega}_o(\tau)}{2} \int_{-1}^{+1} p^o(\mu,\mu') I_g(\tau,\mu') d\mu' \ , \tag{2}$$

with boundary conditions

$$\left.\begin{aligned} I_g(0;-\mu) &= 0 \\ I_g(\tau_b;+\mu) &= B(T_s) \end{aligned}\right\} , \tag{3}$$

where 0 and τ_b denote the cloud top and base, respectively, and T_s is the surface temperature.

For the cloud emission (I_c),

$$\mu \frac{dI_c(\tau;\mu)}{d\tau} = I_c(\tau;\mu) - \frac{\tilde{\omega}_o(\tau)}{2} \int_{-1}^{+1} p^o(\mu,\mu') I_c(\tau;\mu') d\mu'$$

$$- [1 - \tilde{\omega}_o(\tau)] B[T_c(\tau)] \ , \tag{4}$$

with boundary conditions

$$\left.\begin{aligned} I_c(0;-\mu) &= 0 \\ I_c(\tau_b;+\mu) &= 0 \end{aligned}\right\} ; \tag{5}$$

To simplify the expressions, let

$$S'_g(\tau;\mu) = \frac{\tilde{\omega}_o(\tau)}{2} \int_{-1}^{+1} p^o(\mu,\mu') I_g(\tau;\mu') d\mu' \ , \tag{6}$$

and

$$S'_c(\tau;\mu) = \frac{\tilde{\omega}_o(\tau)}{2} \int_{-1}^{+1} p^o(\mu,\mu') I_c(\tau;\mu') d\mu' \ . \qquad (7)$$

Equations (6) and (7) represent the contributions by droplet scatterings. Thus, equations for upward radiation are

$$\mu \frac{dI_g(\tau;+\mu)}{d\tau} = I_g(\tau;+\mu) - S'_g(\tau;+\mu) \ , \qquad (8)$$

and

$$\mu \frac{dI_c(\tau;+\mu)}{d\tau} = I_c(\tau;+\mu) - S'_c(\tau;+\mu) - [1 - \tilde{\omega}_o(\tau)]B[T_c(\tau)], \qquad (9)$$

corresponding to (2) and (4), respectively. Similar expressions can be written for downward radiation by changing $+\mu$ to $-\mu$.

For a finite optical thickness, the expressions are readily solved [20]. The computer program solves (8) and (9) in essentially the same manner by means of the Guass-Seidel iteration technique for upwelling (as well as down-welling) radiation at successive levels from the cloud base to the top in accordance with boundary conditions (3) and (5).

The approximate solutions of (8) and (9) with the boundary conditions specified for the upwelling radiances, I_g and I_c, at each successive level from the cloud base may be written in the form

$$I_g \simeq B_g T + S_g \ , \qquad (10)$$

$$I_c \simeq (1 - \tilde{\omega}_o)B_c(1 - T) + S_c \ , \qquad (11)$$

where B_g represents $B(T_s)$; B_c $B[T_c(\tau)]$; S_g $S'_g(1 - T)$; S_c $S'_c(1 - T)$; and T is the vertical transmittance from the cloud base to that level. Values of I_g and I_c for the cloud model were obtained for 10.5μm, 11.0μm, 11.5μm, 12.0μm, and 12.5μm. The refractive indices for these wavelengths were taken from Irvine and Pollack [21]. The volume scattering, absorption,

and extinction coefficients (per km) for 100 droplets and the average single-scattering albedo for the model cloud are given in Table 2.

Upwelling radiances I_g and I_c together contribute to the total upwelling radiation from the model cloud, whereas I_c represents radiance from an isolated cloud only, i.e., no surface emission contribution [6].

TABLE 2. VOLUME SCATTERING (β_{scat}), ABSORPTION (β_{abs}), AND EXTINCTION (β_{ext}) COEFFICIENTS AND AVERAGE SINGLE SCATTERING ALBEDO ($\tilde{\omega}_o$) OF THE MODEL CLOUD AS A FUNCTION OF WAVELENGTH (λ)

λ (μm)	β_{scat} (km^{-1})	β_{abs} (km^{-1})	β_{ext} (km^{-1})	$\tilde{\omega}_o$
10.5	7.2609	6.1013	13.3622	0.5044
11.0	4.8780	7.2201	12.0981	0.3665
11.5	4.6519	8.5988	13.2507	0.3174
12.0	5.2469	9.7333	14.9802	0.3152
12.5	5.8936	10.3532	16.2468	0.2796

INTERNAL RADIATION STRUCTURE AND DISCUSSIONS

Examination of (10) and (11) reveals that as T becomes closer to unity (or τ approaches 0) near the base of a thick cloud the total upward radiance, $I_g + I_c$, originates mainly from surface radiation and little from cloud emission. On the other hand, near the cloud top where T approaches 0 (or τ approaches infinity), the cloud emission and scattering dominate.

Thus,

$$I_g \simeq 0, \text{ then } I_c \simeq B[T_c(0)] = \overline{B}_c$$

and

$$\overline{B}_c \simeq (1 - \tilde{\omega}_o)B_c + S_c \, . \qquad (12)$$

This means that the apparent blackbody radiation $\overline{B}_c$ at the top of a "black" cloud is composed of two radiant components, which include partly thermal emission and partly scattering. The fractional amount of each is determined by the average single scattering albedo $\tilde{\omega}_o$ of the cloud.

Since the values of all the terms at each level in (10) and (11), except those of S_g and S_c which also include some contributions from downward radiation, can be readily calculated, it is simple to sort out the contributions to the vertical upward radiation made by cloud emission, surface radiation, and droplet scatterings and to examine their changes with wavelength and cloud depth. For simplicity of presentation, the internal cloud radiation field was examined at 100 m intervals up to 500 m as well as the cloud top at 550 m. Also, the cloud model was examined in four different cases involving (1) inhomogeneous droplet and temperature distributions, (2) homogeneous in both droplet and temperature distributions, (3) isothermal but inhomogeneous in droplet distribution, and (4) homogeneous in droplet distribution but with nonisothermal temperature distribution. The first case was run for all the wavelengths listed in the preceding section, and the other three at 10.5μm and 12.5μm only. In this manner, some physical insight may be derived as to the suitability of employing a homogeneous cloud as opposed to an inhomogeneous one for modeling purposes.

Three tables are presented. The first two deal with percentage contributions in the four cases, in which SS denotes the total scattering contributions, i.e., $S_g + S_c$, CE the cloud emission, and TS the reduced surface radiation. To evaluate what role the inclusion of water vapor would play in cloud modeling, the calculated radiance values at each level are given in Table 5, so that the percentage contribution made by water vapor to upward radiation may be understood.

In Table 3, the changes with wavelength of percentage values, when compared with those of optical values in Table 2, show that (1) the surface contributions (TS) at each level vary inversely with the extinction coefficients (β_{ext}), (2) the total scattering contributions (SS) fluctuate about the average single scattering albedos ($\tilde{\omega}_o$) of the cloud, and (3) the emission contributions (CE) increase with the wavelength. An examination of Tables 3 and 4 shows that, at all wavelengths, as the surface contributions decrease with thickness, the emission contributions increase. The scattering contributions due to surface radiation and those due to cloud emission also behave in similar manners, although they are not tabulated here. However, the percentage values of the total scattering contributions in the four cases at corresponding wavelengths are vastly different, except for case 3. This can be explained by the fact that cloud microphysical properties play significant roles in the determination of the internal radiation structures.

TABLE 3. PERCENTAGE CONTRIBUTIONS BY TOTAL SCATTERING (SS), CLOUD EMISSION (CE), AND REDUCED SURFACE RADIATION (TS) TO UPWELLING RADIATION AT DIFFERENT LEVELS (m) AS A FUNCTION OF WAVELENGTH IN CASE 1.

Level (m)		Wavelength(μm) 10.5	11.0	11.5	12.0	12.5
100	SS	44	32	29	32	31
	CE	34	43	49	52	54
	TS	22	25	22	18	15
200	SS	50	36	32	32	32
	CE	40	51	57	60	62
	TS	10	13	11	8	6
300	SS	50	36	32	32	31
	CE	42	54	60	62	65
	TS	8	10	8	6	4
400	SS	50	36	32	32	30
	CE	43	55	61	63	67
	TS	7	9	7	5	3
500	SS	50	36	31	31	28
	CE	44	56	63	65	70
	TS	6	8	6	4	2
550	SS	49	36	31	31	28
	CE	45	58	64	65	70
	TS	6	6	5	4	2

TABLE 4. PERCENTAGE CONTRIBUTIONS BY TOTAL SCATTERING, CLOUD EMISSION, AND REDUCED SURFACE RADIATION TO UPWELLING RADIATION AT DIFFERENT LEVELS AT 10.5μm AND 12.5μm IN CASE 2 (HOMO DT), CASE 3 (HOMO T ONLY), AND CASE 4 (HOMO D ONLY).

Level(m)		Case 2 Homo DT(μm) 10.50	12.50	Case 3 Homo T Only(μm) 10.50	12.50	Case 4 Homo D Only(μm) 10.50	12.50
100	SS	23	17	44	31	23	17
	CE	17	32	34	54	17	32
	TS	60	51	22	15	60	51
200	SS	36	25	50	32	36	25
	CE	28	49	39	62	28	49
	TS	36	26	11	6	36	26
300	SS	34	29	51	31	34	29
	CE	29	58	41	65	30	59
	TS	37	13	8	4	36	12
400	SS	48	31	50	30	48	31
	CE	39	63	43	67	39	63
	TS	13	6	7	3	13	6
500	SS	51	31	50	28	50	31
	CE	42	66	44	70	42	66
	TS	7	3	6	2	8	3
550	SS	51	32	49	28	51	31
	CE	43	66	45	70	43	67
	TS	6	2	6	2	6	2

TABLE 5. PERCENTAGE EFFECT OF WATER VAPOR ON UPWELLING RADIATION AT DIFFERENT LEVELS AS A FUNCTION OF WAVELENGTH.

Level (m)	Vapor	10.50 λ(μm)	11.00 λ(μm)	11.50 λ(μm)	12.00 λ(μm)	12.50 λ(μm)
100	Yes	89.34	95.60	100.9	105.8	110.2
	No	89.49	95.77	101.1	106.0	110.7
	Percentage	-0.2	-0.2	-0.2	-0.2	-0.4
200	Yes	86.48	92.76	98.14	103.1	107.6
	No	86.67	92.96	98.33	103.3	108.0
	Percentage	-0.2	-0.2	-0.2	-0.2	-0.4
300	Yes	85.52	91.84	97.27	102.3	106.8
	No	85.78	92.11	97.51	102.5	107.2
	Percentage	-0.3	-0.3	-0.2	-0.2	-0.4
400	Yes	84.88	91.21	96.66	101.7	106.1
	No	85.20	91.55	96.95	102.0	106.7
	Percentage	-0.4	-0.4	-0.3	-0.3	-0.6
500	Yes	84.41	90.75	96.20	101.2	105.5
	No	84.79	91.15	96.56	101.6	106.3
	Percentage	-0.4	-0.4	-0.4	-0.4	-0.8
550	Yes	84.23	90.58	96.03	101.1	105.3
	No	84.64	91.01	96.42	101.4	106.1
	Percentage	-0.5	-0.5	-0.4	-0.4	-0.8

Percentage contributions are almost identical at corresponding levels at both the 10.5μm and 12.5μm wavelengths in cases 1 and 3 which share the same inhomogeneous droplet distribution. The percentage values are nearly identical in cases 2 and 4 which share the same homogeneous droplet distribution. Apparently, this indicates that the upward radiation emerging from any level inside as well as at the top of a cloud is virtually independent of its internal temperature structure; moreover, this implies that the so-called cloud-top temperature may be regarded as the mean temperature of the cloud.

When the cloud is viewed as a whole, i.e., 550 m in thickness, the amounts in all four cases of upward radiation emerging from the top are nearly the same at their corresponding wavelengths. The calculated radiance values are 84.23, 83.85, 83.95, and 83.67 mW m^{-2} sr^{-1} cm at 10.5μm for the four cases, respectively. At 12.5μm, they are 105.30, 105.50, 105.70, and 104.85, respectively. Thus considering the cloud as a whole, little difference exists at a given wavelength in upward radiation emerging from its top between a homogeneous model and an inhomogeneous one so long as they have the same total droplet number or the same total liquid water amount and the same mean temperature in the cloud column.

In the present study, since surface emission (TS) still contributes to the upward radiance at the cloud top, the cloud is not "black." It is even less black at 10.5μm than at 12.5μm. The calculated average cloud vertical emissivity over the 10.5μm to 12.5μm interval is 0.85 compared with Platt's value [15] of about 0.90 in the 10μm to 12μm band. Furthermore, it may be observed in Table 3 that at the 550 m level the scattering contributions (SS) at all wavelengths nearly equal the average single scattering albedos of the cloud in Table 2 at the corresponding wavelengths. If the cloud were to grow another 200 to 300 m thicker, it could be expected, as indicated in (12), that at 10.5μm, for example, the upward emission and scattering contributions would split about 50-50. And this is when cloud emissivity would reach about unity.

Table 5 shows the effect of water vapor on upward radiation at different levels as a function of wavelength. Although there was appreciable water vapor inside the cloud with about 98% relative humidity on the average as given in Table 1, the presence of water vapor appears to have negative but negligible effects on the upward radiance.

RATIO TEST OF CLOUD BLACKNESS

Not until a cloud behaves like a blackbody radiator can the study of its internal radiation field ignore the radiation contribution from the underlying surface. The surface temperature is, in general, appreciably higher than the cloud temperature, while the cloud-top temperature is lower than the base temperature. Only when the cloud becomes "black" will the upwelling radiation directly relate to the cloud-top temperature. For a nonblack cloud, the cloud radiation field is contaminated by the surface radiation; one might say that the radiation field is distorted. To illustrate such distortion, Table 6 shows the equivalent blackbody temperatures of the radiation field at different levels as a function of wavelength.

TABLE 6. EQUIVALENT BLACKBODY TEMPERATURES (°C) CORRESPONDING TO UPWELLING RADIANCES AS A FUNCTION OF WAVELENGTH AT DIFFERENT LEVELS FROM THE CLOUD BASE WITH MEAN TEMPERATURES ($\bar{T}$ °C).

Level (m)	$\bar{T}$ (°C)	10.50 (μm)	11.00 (μm)	11.50 (μm)	12.00 (μm)	12.50 (μm)
100	9.13	15.03	14.34	13.50	12.88	12.37
200	9.19	13.08	12.47	11.72	11.15	10.72
300	9.06	12.42	11.85	11.15	10.63	10.20
400	8.84	11.98	11.43	10.75	10.24	9.75
500	8.62	11.65	11.12	10.44	9.92	9.37
550	8.52	11.53	11.00	10.33	9.85	9.24

Even though the mean temperature at a given level is at a constant temperature, the equivalent blackbody temperatures decrease with wavelength. Normally, blackbody radiance values increase monotonically with wavelength at a given temperature. In the present situation, the radiance values at a given level in Table 5 also increase; however, the amount of increase is relatively small. The percentage increases in blackbody radiance at, for instance, 9°C are about 9%, 17%, 24%, and 30%, and at 14°C about 8%, 16%, 22%, and 28%, respectively, for 11.0μm, 11.5μm, 12.0μm, and 12.5μm, with reference to the blackbody value for 10.5μm. By comparison, the percentage increases in Table 5 at, for instance, the 100-m level are about 7%, 13%, 18%, and 23%, respectively. At the 550-m level, they are about 8%, 14%, 20%, and 25%, respectively. It is this distortion of the temperature-wavelength relationship, or rather of the radiance-wavelength relationship inside the cloud, that forms the basis upon which the proposed method for determining the quality of cloud blackness or, to some extent, cloud emissivity is developed.

Tables 3 and 6 show an apparent excess in the amount of vertical upward radiation, more at 10.5μm than at any other wavelengths, giving rise to higher equivalent blackbody temperatures in Table 6 at all levels. On the other hand, Table 3 appears to indicate that the surface (TS) and hence the resulting scattering contributions (SS) together are somewhat greater at 10.5μm.

The former is governed by the extinction coefficient of the cloud and the latter by its single scattering albedo. If the ratio of the observed radiance at 10.5μm to that at a longer wavelength in the same window region is taken, this ratio will enhance the presence of an excessive amount at 10.5μm of surface and scattered radiation when the cloud is not "black." However, when the cloud is "black," i.e., no contribution from surface and scattered radiation, the ratio would be equivalent to

that of blackbody radiances. Table 7 gives the ratios of blackbody radiances as a function of temperature. The 11.0μm wavelength was not used, not only because it lies too close to the 10.5μm wavelength, but also because the advantage of its lower single scattering albedo is somewhat offset by the disadvantage of its lower extinction coefficient. On the basis of these discussions, the two criteria for choosing the shorter wavelength are: (1) relatively higher single scattering albedo and (2) relatively lower extinction coefficient. The 11.0μm wavelength satisfies (2) but not quite (1), as indicated in Table 2.

TABLE 7. RATIOS OF BLACKBODY RADIANCES AT TWO WAVELENGTHS AS A FUNCTION OF AIR TEMPERATURE (°C)

Temperature (°C)	Wavelength Ratio		
	10.5/11.5	10.5/12.0	10.5/12.5
-25.0	0.8108	0.7455	0.6934
-20.0	0.8184	0.7555	0.7053
-15.0	0.8257	0.7652	0.7168
-10.0	0.8327	0.7746	0.7281
-5.0	0.8396	0.7838	0.7391
0.0	0.8462	0.7927	0.7499
5.0	0.8527	0.8014	0.7604
10.0	0.8589	0.8098	0.7706
15.0	0.8650	0.8180	0.7806
20.0	0.8709	0.8260	0.7903
25.0	0.8766	0.8337	0.7998
30.0	0.8821	0.8413	0.8090
35.0	0.8875	0.8487	0.8181

When the cloud in question is "black" in the window region, the ratio of the observed radiances will give the cloud temperature. Moreover, only under this condition will the radiance values at the two wavelengths, upon conversion, also yield nearly the same temperature. The ratio of blackbody radiances in Table 7 changes rather slowly with temperature within narrow limits, and it does not take many extra surface and scattering contributions to cause the ratio to deviate appreciably from its critical blackbody value. The critical ratio is unknown; but since the primary interest lies in establishing a reliability criterion for accepting or rejecting the temperature derived from satellite data, the problem is to find a means to distinguish between black and nonblack clouds. For this purpose, a reference ratio instead of the critical ratio is sought.

Besides the present cloud model, a number of homogeneous models such as those used by Yamamoto et al. [5] and Hunt [8] were also investigated. They were 1 km thick. After repeated numerical experiments, it was found

that the ratio of the blackbody radiances derived from the surface temperature served quite well as a reference ratio. When the ratio of the observed (or more appropriately, synthetic) radiances at a certain cloud level became smaller than the reference ratio, the calculated vertical emissivity at that level in every case showed better than 0.95 in the window region. The surface temperature need not be accurate. Since most clouds, except those low-hanging stratus and fogs, are generally 1 km or more above the ground, a temperature 10 degrees less than the estimated surface temperature could be used. Over the continent, even lower temperatures could be used. This approach was tested for 10 degrees less; and an improvement of about 1%-2% was obtained.

To illustrate the technique just described for determining the degree of cloud blackness or cloud emissivity, Tables 8 and 9 may serve as examples. Table 8 shows the inhomogeneous model, and Table 9 one of Yamamoto's [5] homogeneous clouds. This particular cloud given here had a surface temperature of 30°C and a cloud temperature of -30°C.

In the case of Platt's [15] cloud in Table 8, the cloud never becomes "black" since the observed ratios at any levels never become smaller than their respective reference ratios, although at 550 m the former nearly approach the latter. In Table 9 the ratios are tabulated up to 550 m as well as at 1 km, the top of the model cloud. The reference ratios at 30°C can also be directly obtained from Table 7. The "observed" ratios at the cloud top, when compared with the corresponding values in Table 7, indicate that the equivalent cloud temperature is below -25°C, which is compatible with the given cloud temperature of the model. These ratios are appreciably smaller than the reference ratios. The small arrows in Table 9 show where the "observed" ratios become smaller. It is evident that they occur at different levels, 450 m, 500 m, and 550 m. Past studies [6] show that cloud emissivity (or blackness) is frequency-dependent. Hence, a nonblack cloud at 10.5μm may appear "black" when viewed at 12.0μm or 12.5μm, which means that if cloud emissivity is required to be the same in this window region then the required cloud thickness will decrease as wavelength increases. To further illuminate this point, the calculated vertical emissivities at these three levels are listed as a function of wavelength:

Level (m)	Wavelength(μm)				
	10.5	11.0	11.5	12.0	12.5
450	0.90	0.93	0.96	0.97	0.97
500	0.92	0.95	0.97	0.98	0.98
550	0.94	0.96	0.98	0.99	0.99

TABLE 8. RATIOS OF THE "OBSERVED" RADIANCES AT DIFFERENT LEVELS OF THE INHOMOGENEOUS CLOUD MODEL (SURFACE TEMPERATURE = 21.70°C)

Level (m)	Wavelength Ratio		
	10.5/11.5	10.5/12.0	10.5/12.5
550	0.8771	0.8331	0.7999
500	0.8774	0.8341	0.8001
450	0.8778	0.8338	0.7999
400	0.8781	0.8346	0.8000
350	0.8787	0.8351	0.8006
300	0.8792	0.8360	0.8007
250	0.8801	0.8369	0.8018
200	0.8812	0.8388	0.8037
150	0.8828	0.8408	0.8408
100	0.8854	0.8444	0.8107
50	0.8848	0.8440	0.8110
Surface	0.8728	0.8285	0.7935

Note: The last row contains the reference ratios.

TABLE 9. RATIOS OF THE "OBSERVED" RADIANCES AT DIFFERENT LEVELS OF THE HOMOGENEOUS CLOUD MODEL (SURFACE TEMPERATURE = 30°C AND CLOUD TEMPERATURE = -30°C)

Level (m)	Wavelength Ratio		
	10.5/11.5	10.5/12.0	10.5/12.5
1000	0.8101	0.7425	0.6878
550	→0.8726	0.8134	0.7585
500	0.8895	→0.8344	0.7802
450	0.9088	0.8593	→0.8066
400	0.9297	0.8877	0.8376
350	0.9511	0.9181	0.8719
300	0.9706	0.9481	0.9072
250	0.9835	0.9729	0.9385
200	0.9913	0.9865	0.9586
150	0.9852	0.9825	0.9596
100	0.9648	0.9565	0.9345
50	0.9299	0.9083	0.8820
Surface	0.8821	0.8413	0.8090

Note: Small arrow points to where the observed ratio becomes less than the reference ratio.

The last row contains the reference ratios.

If straight averages are taken on the emissivity values, for the 450 m, 500 m, and 550 m levels, the emissivity values are 0.95, 0.96, and 0.97, respectively. At 550 m Yamamoto's cloud appeared "blacker" than Platt's. Although the former had a size range from 0.01μm to 10.0μm and the latter a size range from 0.5μm to 25.0μm, Yamamoto used an averaged value of 100 cm^{-3} per level in number concentration or 0.063 g m^{-3} in liquid water content, whereas Platt had a value of only 40 cm^{-3} or a liquid content of 0.035 g m^{-3}.

SUMMARY AND CONCLUSIONS

In this study, a detailed investigation was performed in the 10.5μm to 12.5μm window region of the internal structure of the vertical upward radiation emerging from the different levels inside a realistic inhomogeneous cloud in the hope to derive additional physical insight for an understanding of cloud radiation. The contributions to the internal radiation field consists of two components: one includes the thermal emission of cloud particles and water vapor and the resulting Mie scattering by these particles, and the other includes the thermal emission from the ground or sea surface and the resulting scattering. As the former increases with cloud depth, the latter decreases. When both are present, the cloud is not "black" and its radiation field is said to be distorted by the penetration of surface radiation and scattering. Such penetration is greater at 10.5μm than at longer wavelengths. When the penetration ceases, the cloud emission and scattering completely dominate the radiation field and the cloud then behaves like a blackbody radiator. The fractional amounts of thermal emission and scattering contributing to the blackbody radiation at the cloud top are determined by the average single scattering albedo of the cloud.

The average meteorological and microphysical properties were utilized to examine clouds of various homogeneous states at two wavelengths for their internal radiation fields. The microphysical property of clouds was shown to be of prime importance in cloud modeling, whereas the temperature distribution within the cloud had little effect on either the upwelling radiation from the cloud top or the internal radiation distribution.

From such detailed investigation, a technique was evolved which takes advantage of the distorted radiation field in a cloud. A 10.5μm channel is proposed in addition to the existing window channel in the 12μm window region in satellite sounders. The ratio of the observed upward radiances at these two wavelengths, when compared with that of the blackbody radiances derived for the corresponding wavelengths from a knowledge of the surface temperature, which could be an estimate, offers a good indication of the degree of the cloud blackness or of cloud emissivity. Consequently, it appears possible to determine the reliability of the temperature field derived from satellite data. It was shown that the technique for distinguishing the cloud blackness does not require an accurate surface temperature. Two examples were presented in which one cloud was not so "black"

and the other was. The clouds which have satisfied the ratio test at different levels normally have emissivity values about 0.95 or more. On the other hand, when the observed upward radiances, upon conversion to temperature, give nearly the same value, cloud emissivity may be taken to be unity and that temperature then the cloud-top temperature.

Finally, this proposed technique is simple and inexpensive to execute on board a satellite. Moreover, the ratio test minimizes the systematic errors, which are found in all measuring devices and which are difficult to account for.

REFERENCES

1. Glahn, H. R., 1966, "On the Usefulness of Satellite Infrared Measurements in Determination of Cloud Top Heights and Areal Coverage." J. Appl. Meteor., 5:189-197.

2. Chahine, M. T., 1974, "Remote Sounding of Cloudy Atmospheres: I. The Single Cloud Layer." J. Atmos. Sci., 31:233-243.

3. Chahine, M. T., 1977, "Remote Sounding of Cloudy Atmospheres: II. Multiple Cloud Formations." J. Atmos. Sci., 34:744-757.

4. Chahine, M. T., H. H. Aumann, and F. W. Taylor, 1977, "Remote Sounding of Cloudy Atmospheres: III. Experimental Verifications." J. Atmos. Sci., 34:758-765.

5. Yamamoto, G. M. Tanaka, and K. Kamitani, 1966, "Radiative Transfer in Water Clouds in the 10μm Window Region." J. Atmos. Sci., 23:305-313.

6. Zdunkowski, W. G., and I. Choronenko, 1969, "Incomplete Blackness of Clouds in the Infrared Spectrum." Contr. Atmos. Phys., 42:206-224.

7. Yamamoto, G. M. Tanaka, K. Kamitani, and S. Asano, 1970, "Radiative Transfer in Water Clouds in the Infrared Region." J. Atmos. Sci., 27:282-292.

8. Hunt, G. E., 1973, "Radiative Properties of Terrestrial Clouds at Visible and Infrared Thermal Window Wavelengths." Quart. J. Roy. Meteor. Soc., 99:346-369.

9. Herman, B. M., and S. R. Browning, 1965, "A Numerical Solution to the Equation of Radiative Transfer." J. Atmos. Sci., 22:559-566.

10. Low, R. D. H., 1977, "Effects of Cloud Particles on Remote Sensing from Space in the 10μm Infrared Region." R&D Report, ECOM-5811 (AD-A038502), Atmospheric Sciences Laboratory, US Army Electronics Command, White Sands Missile Range, NM.

11. Selby, J. E. A., and R. A. McClatchey, 1975, "Atmospheric Transmittance from 0.25μm to 28.5μm: Computer Code LOWTRAN 3." Environ. Res. Pap., No. 513 (AFCRL-TR-75-0255), AF Cambridge Res. Labs., Hanscom AFB, MA.

12. Roberts, R. E., J. E. A. Selby, and L. M. Bierman, 1976, "Infrared Continuum Absorption by Atmospheric Water Vapor in the 8μm-12μm Window." Appl. Op., 15:2085-2090.

13. Stephens, G. L., 1976, "The Transfer of Radiation Through Vertically Non-Uniform Stratocumulus Water Clouds." Contr. Atmos. Phys., 49:237-253.

14. Paltridge, G. W., 1974, "Infrared Emissivity, Short-Wave Albedo, and the Microphysics of Stratiform Water Clouds." J. Geophys. Res., 79:4053-4058.

15. Platt, C. M. R., 1972, "Airborne Infrared Radiance Measurements (10μm-12μm) off Tropical East-Coast Australia." J. Geophys. Res., 77:1597-1609.

16. Fletcher, N. H., 1962, The Physics of Rainclouds, Cambridge Univ. Press, Cambridge.

17. Borovikov, A. M., and A. Kh. Khrgian, 1963, Cloud Physics, Israel Program for Scientific Translations, Jerusalem.

18. Mason, B. J., 1971, The Physics of Clouds. Clarendon Press, Oxford.

19. Levine, L. M., 1958, "Functions to Represent Drop Size Distributions in Clouds: The Optical Density of Clouds." Izv. Geofiz. Ser., 10:1211-1221. (translation).

20. Chandrasekhar, S., 1960, Radiative Transfer. Dover, NY.

21. Irvine, W. M., and J. B. Pollack, 1968, "Infrared Optical Properties of Water and Ice Spheres." Icarus, 8:324-360.

DISTRIBUTION LIST

Director
US Army Ballistic Research Laboratory
ATTN: DRDAR-BLB, Dr. G. E. Keller
Aberdeen Proving Ground, MD 21005

Air Force Weapons Laboratory
ATTN: Technical Library (SUL)
Kirtland AFB, NM 87117

Commander
Headquarters, Fort Huachuca
ATTN: Tech Ref Div
Fort Huachuca, AZ 85613

6585 TG/WE
Holloman AFB, NM 88330

Commandant
US Army Field Artillery School
ATTN: Morris Swett Tech Library
Fort Sill, OK 73503

Commandant
USAFAS
ATTN: ATSF-CD-MT (Mr. Farmer)
Fort Sill, OK 73503

Director
US Army Engr Waterways Exper Sta
ATTN: Library Branch
Vicksburg, MS 39180

Commander
US Army Electronics Command
ATTN: DRSEL-CT-S (Dr. Swingle)
Fort Monmouth, NJ 07703
03

CPT Hugh Albers, Exec Sec
Interdept Committee on Atmos Sci
Fed Council for Sci & Tech
National Sci Foundation
Washington, DC 20550

Inge Dirmhirn, Professor
Utah State University, UMC 48
Logan, UT 84322

HQDA (DAEN-RDM/Dr. De Percin)
Forrestal Bldg
Washington, DC 20314

Commander
US Army Aviation Center
ATTN: ATZQ-D-MA
Fort Rucker, AL 36362

CO, USA Foreign Sci & Tech Center
ATTN: DRXST-ISI
220 7th Street, NE
Charlottesville, VA 22901

Director
USAE Waterways Experiment Station
ATTN: Library
PO Box 631
Vicksburg, MS 39180

US Army Research Office
ATTN: DRXRO-IP
PO Box 12211
Research Triangle Park, NC 27709

Mr. William A. Main
USDA Forest Service
1407 S. Harrison Road
East Lansing, MI 48823

Library-R-51-Tech Reports
Environmental Research Labs
NOAA
Boulder, CO 80302

Commander
US Army Dugway Proving Ground
ATTN: MT-S
Dugway, UT 84022

HQ, ESD/DRI/S-22
Hanscom AFB
MA 01731

Head, Atmospheric Rsch Section
National Science Foundation
1800 G. Street, NW
Washington, DC 20550

Office, Asst Sec Army (R&D)
ATTN: Dep for Science & Tech
HQ, Department of the Army
Washington, DC 20310

Commander
US Army Satellite Comm Agc
ATTN: DRCPM-SC-3
Fort Monmouth, NJ 07703

Sylvania Elec Sys Western Div
ATTN: Technical Reports Library
PO Box 205
Mountain View, CA 94040

William Peterson
Research Association
Utah State University, UNC 48
Logan, UT 84322

Defense Communications Agency
Technical Library Center
Code 205
Washington, DC 20305

Dr. A. D. Belmont
Research Division
PO Box 1249
Control Data Corp
Minneapolis, MN 55440

Commander
US Army Electronics Command
ATTN: DRSEL-WL-D1
Fort Monmouth, NJ 07703

Commander
ATTN: DRSEL-VL-D
Fort Monmouth, NJ 07703

Meteorologist in Charge
Kwajalein Missile Range
PO Box 67
APO
San Francisco, CA 96555

The Library of Congress
ATTN: Exchange & Gift Div
Washington, DC 20540
2

US Army Liaison Office
MIT-Lincoln Lab, Library A-082
PO Box 73
Lexington, MA 02173

Dir National Security Agency
ATTN: TDL (C513)
Fort George G. Meade, MD 20755

Director, Systems R&D Service
Federal Aviation Administration
ATTN: ARD-54
2100 Second Street, SW
Washington, DC 20590

Commander
US Army Missile Command
ATTN: DRSMI-RRA, Bldg 7770
Redstone Arsenal, AL 35809

Dir of Dev & Engr
Defense Systems Div
ATTN: SAREA-DE-DDR
H. Tannenbaum
Edgewood Arsenal, APG, MD 21010

Naval Surface Weapons Center
Technical Library & Information
Services Division
White Oak, Silver Spring, MD
20910

Dr. Frank D. Eaton
PO Box 3038
Universtiy Station
Laramie, Wyoming 82071

Rome Air Development Center
ATTN: Documents Library
TILD (Bette Smith)
Griffiss Air Force Base, NY 13441

National Weather Service
National Meteorological Center
World Weather Bldg - 5200 Auth Rd
ATTN: Mr. Quiroz
Washington, DC 20233

USAFETAC/CB (Stop 825)
Scott AFB
IL 62225

Director
Defense Nuclear Agency
ATTN: Tech Library
Washington, DC 20305

Director
Development Center MCDEC
ATTN: Firepower Division
Quantico, VA 22134

Environmental Protection Agency
Meteorology Laboratory
Research Triangle Park, NC
27711

Commander
US Army Electronics Command
ATTN: DRSEL-GG-TD
Fort Monmouth, NJ 07703

Commander
US Army Ballistic Rsch Labs
ATTN: DRXBR-IB
APG, MD 21005

Dir, US Naval Research Lab
Code 5530
Washington, DC 20375

Mil Assistant for
Environmental Sciences
DAD (E & LS), 3D129
The Pentagon
Washington, DC 20301

The Environmental Rsch
Institute of MI
ATTN: IRIA Library
PO Box 618
Ann Arbor, MI 48107

Armament Dev & Test Center
ADTC (DLOSL)
Eglin AFB, Florida 32542

Range Commanders Council
ATTN: Mr. Hixon
PMTC Code 3252
Pacific Missile Test Center
Point Mugu, CA 93042

Commander
Eustis Directorate
US Army Air Mobility R&D Lab
ATTN: Technical Library
Fort Eustis, VA 23604

Commander
Frankford Arsenal
ATTN: SARFA-FCD-O, Bldg 201-2
Bridge & Tarcony Sts
Philadelphia, PA 19137

Director, Naval Oceanography and
Meteorology
National Space Technology Laboratories
Bay St Louis, MS 39529

Commander
US Army Electronics Command
ATTN: DRSEL-CT-S
Fort Monmouth, NJ 07703

Commander
USA Cold Regions Test Center
ATTN: STECR-OP-PM
APO Seattle 98733

Redstone Scientific Information Center
ATTN: DRDMI-TBD
US Army Missile Res & Dev Command
Redstone Arsenal, AL 35809

Commander
AFWL/WE
Kirtland AFB, NM 87117

Naval Surface Weapons Center
Code DT-22 (Ms. Greeley)
Dahlgren, VA 22448

Commander
Naval Ocean Systems Center
ATTN: Research Library
San Diego, CA 92152

Commander
US Army INSCOM
ATTN: IARDA-OS
Arlington Hall Station
Arlington, VA 22212

Commandant
US Army Field Artillery School
ATTN: ATSF-CF-R
Fort Sill, OK 73503

Commander and Director
US Army Engineer Topographic Labs
ETL-GS-AC
Fort Belvoir, VA 22060

Technical Processes Br-D823
NOAA, Lib & Info Serv Div
6009 Executive Blvd
Rockville, MD 20852

Commander
US Army Missile Research
and Development Command
ATTN: DRDMI-CGA, B. W. Fowler
Redstone Arsenal, AL 35809

Commanding Officer
US Army Armament Rsch & Dev Com
ATTN: DRDAR-TSS #59
Dover, NJ 07801

Air Force Cambridge Rsch Labs
ATTN: LCB (A. S. Carten, Jr.)
Hanscom AFB
Bedford, MA 01731

National Center for Atmos Res
NCAR Library
PO Box 3000
Boulder, CO 80307

Air Force Geophysics Laboratory
ATTN: LYD
Hanscom AFB
Bedford, MA 01731

Chief, Atmospheric Sciences Division
Code ES-81
NASA
Marshall Space Flight Center, AL 35812

Department of the Air Force
OL-C, 5WW
Fort Monroe, VA 23651

Commander
US Army Missile Rsch & Dev Com
ATTN: DRDMI-TR
Redstone Arsenal, AL 35809

Meteorology Laboratory
AFGL/LY
Hanscom AFB, MA 01731

Director CFD
US Army Field Artillery School
ATTN: Met Division
Fort Sill, OK 73503

Naval Weapons Center (Code 3173)
ATTN: Dr. A. Shlanta
China Lake, CA 93555

Director
Atmospheric Physics & Chem Lab
Code R31, NOAA
Department of Commerce
Boulder, CO 80302

Department of the Air Force
5 WW/DN
Langley AFB, VA 23665

Commander
US Army Intelligence Center and School
ATTN: ATSI-CD-MD
Fort Huachuca, AZ 85613

Dr. John L. Walsh
Code 4109
Navy Research Lab
Washington, DC 20375

Director
US Army Armament Rsch & Dev Com
Chemical Systems Laboratory
ATTN: DRDAR-CLJ-I
Aberdeen Proving Ground, MD 21010

R. B. Girardo
Bureau of Reclamation
E&R Center, Code 1220
Denver Federal Center, Bldg 67
Denver, CO 80225

Commander
US Army Missile Command
ATTN: DRDMI-TEM
Redstone Arsenal, AL 35809

Commander
US Army Tropic Test Center
ATTN: STETC-MO (Tech Library)
APO New York 09827

Commanding Officer
Naval Research Laboratory
Code 2627
Washington, DC 20375

Defense Documentation Center
ATTN: DDC-TCA
Cameron Station (Bldg 5)
Alexandria, Virginia 22314
12

Commander
US Army Test and Evaluation Command
ATTN: Technical Library
White Sands Missile Range, NM 88002

US Army Nuclear Agency
ATTN: MONA-WE
Fort Belvoir, VA 22060

Commander
US Army Proving Ground
ATTN: Technical Library
Bldg 2100
Yuma, AZ 85364

Office, Asst Sec Army (R&D)
ATTN: Dep for Science & Tech
HQ, Department of the Army
Washington, DC 20310

ATMOSPHERIC SCIENCES RESEARCH PAPERS

1. Lindberg, J.D., "An Improvement to a Method for Measuring the Absorption Coefficient of Atmospheric Dust and other Strongly Absorbing Powders, " ECOM-5565, July 1975.
2. Avara, Elton, P., "Mesoscale Wind Shears Derived from Thermal Winds," ECOM-5566, July 1975.
3. Gomez, Richard B., and Joseph H. Pierluissi, "Incomplete Gamma Function Approximation for King's Strong-Line Transmittance Model," ECOM-5567, July 1975.
4. Blanco, A.J., and B.F. Engebos, "Ballistic Wind Weighting Functions for Tank Projectiles," ECOM-5568, August 1975.
5. Taylor, Fredrick J., Jack Smith, and Thomas H. Pries, "Crosswind Measurements through Pattern Recognition Techniques," ECOM-5569, July 1975.
6. Walters, D.L., "Crosswind Weighting Functions for Direct-Fire Projectiles," ECOM-5570, August 1975.
7. Duncan, Louis D., "An Improved Algorithm for the Iterated Minimal Information Solution for Remote Sounding of Temperature," ECOM-5571, August 1975.
8. Robbiani, Raymond L., "Tactical Field Demonstration of Mobile Weather Radar Set AN/TPS-41 at Fort Rucker, Alabama," ECOM-5572, August 1975.
9. Miers, B., G. Blackman, D. Langer, and N. Lorimier, "Analysis of SMS/GOES Film Data," ECOM-5573, September 1975.
10. Manquero, Carlos, Louis Duncan, and Rufus Bruce, "An Indication from Satellite Measurements of Atmospheric CO2 Variability," ECOM-5574, September 1975.
11. Petracca, Carmine, and James D. Lindberg, "Installation and Operation of an Atmospheric Particulate Collector," ECOM-5575, September 1975.
12. Avara, Elton P., and George Alexander, "Empirical Investigation of Three Iterative Methods for Inverting the Radiative Transfer Equation," ECOM-5576, October 1975.
13. Alexander, George D., "A Digital Data Acquisition Interface for the SMS Direct Readout Ground Station — Concept and Preliminary Design," ECOM-5577, October 1975.
14. Cantor, Israel, "Enhancement of Point Source Thermal Radiation Under Clouds in a Nonattenuating Medium," ECOM-5578, October 1975.
15. Norton, Colburn, and Glenn Hoidale, "The Diurnal Variation of Mixing Height by Month over White Sands Missile Range, N.M," ECOM-5579, November 1975.
16. Avara, Elton P., "On the Spectrum Analysis of Binary Data," ECOM-5580, November 1975.
17. Taylor, Fredrick J., Thomas H. Pries, and Chao-Huan Huang, "Optimal Wind Velocity Estimation," ECOM-5581, December 1975.
18. Avara, Elton P., "Some Effects of Autocorrelated and Cross-Correlated Noise on the Analysis of Variance, " ECOM-5582, December 1975.
19. Gillespie, Patti S., R.L. Armstrong, and Kenneth O. White, "The Spectral Characteristics and Atmospheric CO2 Absorption of the Ho^{+3}:YLF Laser at 2.05μm," ECOM-5583, December 1975.
20. Novlan, David J. "An Empirical Method of Forecasting Thunderstorms for the White Sands Missile Range," ECOM-5584, February 1976.
21. Avara, Elton P., "Randomization Effects in Hypothesis Testing with Autocorrelated Noise," ECOM-5585, February 1976.
22. Watkins, Wendell R., "Improvements in Long Path Absorption Cell Measurement," ECOM-5586, March 1976.
23. Thomas, Joe, George D. Alexander, and Marvin Dubbin, "SATTEL — An Army Dedicated Meteorological Telemetry System," ECOM-5587. March 1976.
24. Kennedy, Bruce W., and Delbert Bynum, "Army User Test Program for the RDT&E-XM-75 Meteorological Rocket," ECOM-5588, April 1976.

25. Barnett, Kenneth M., "A Description of the Artillery Meteorological Comparisons at White Sands Missle Range, October 1974 - December 1974 ('PASS' - Prototype Artillery [Meteorological] Subsystem)," ECOM-5589, April 1976.
26. Miller, Walter B., "Preliminary Analysis of Fall-of-Shot From Project 'PASS'," ECOM-5590, April 1976.
27. Avara, Elton P., "Error Analysis of Minimum Information and Smith's Direct Methods for Inverting the Radiative Transfer Equation," ECOM-5591, April 1976.
28. Yee, Young P., James D. Horn, and George Alexander, "Synoptic Thermal Wind Calculations from Radiosonde Observations Over the Southwestern United States," ECOM-5592, May 1976.
29. Duncan, Louis D., and Mary Ann Seagraves, "Applications of Empirical Corrections to NOAA-4 VTPR Observations," ECOM-5593, May 1976.
30. Miers, Bruce T., and Steve Weaver, "Applications of Meterological Satellite Data to Weather Sensitive Army Operations,"ECOM-5594, May 1976.
31. Sharenow, Moses, "Redesign and Improvement of Balloon ML-566," ECOM-5595, June, 1976.
32. Hansen, Frank V., "The Depth of the Surface Boundary Layer," ECOM-5596, June 1976.
33. Pinnick, R.G., and E.B. Stenmark, "Response Calculations for a Commercial Light-Scattering Aerosol Counter," ECOM-5597, July 1976.
34. Mason, J., and G.B. Hoidale, "Visibility as an Estimator of Infrared Transmittance," ECOM-5598, July 1976.
35. Bruce, Rufus E., Louis D. Duncan, and Joseph H. Pierluissi, "Experimental Study of the Relationship Between Radiosonde Temperatures and Radiometric-Area Temperatures," ECOM-5599, August 1976.
36. Duncan, Louis D., "Stratospheric Wind Shear Computed from Satellite Thermal Sounder Measurements," ECOM-5800, September 1976.
37. Taylor, F., P. Mohan, P. Joseph and T. Pries, "An All Digital Automated Wind Measurement System," ECOM-5801, September 1976.
38. Bruce, Charles, "Development of Spectrophones for CW and Pulsed Radiation Sources," ECOM-5802, September 1976.
39. Duncan, Louis D., and Mary Ann Seagraves,"Another Method for Estimating Clear Column Radiances," ECOM-5803, October 1976.
40. Blanco, Abel J., and Larry E. Taylor, "Artillery Meteorological Analysis of Project Pass," ECOM-5804, October 1976.
41. Miller, Walter, and Bernard Engebos," A Mathematical Structure for Refinement of Sound Ranging Estimates," ECOM-5805, November, 1976.
42. Gillespie, James B., and James D. Lindberg, "A Method to Obtain Diffuse Reflectance Measurements from 1.0 to 3.0 μm Using a Cary 17I Spectrophotometer," ECOM-5806, November 1976.
43. Rubio, Roberto, and Robert O. Olsen,"A Study of the Effects of Temperature Variations on Radio Wave Absorption,"ECOM-5807, November 1976.
44. Ballard, Harold N., "Temperature Measurements in the Stratosphere from Balloon-Borne Instrument Platforms, 1968-1975," ECOM-5808, December 1976.
45. Monahan, H.H., "An Approach to the Short-Range Prediction of Early Morning Radiation Fog," ECOM-5809, January 1977.
46. Engebos, Bernard Francis, "Introduction to Multiple State Multiple Action Decision Theory and Its Relation to Mixing Structures," ECOM-5810, January 1977.
47. Low, Richard D.H.,"Effects of Cloud Particles on Remote Sensing from Space in the 10-Micrometer Infrared Region," ECOM-5811, January 1977.
48. Bonner, Robert S., and R. Newton, "Application of the AN/GVS-5 Laser Rangefinder to Cloud Base Height Measurements," ECOM-5812, February 1977.

49. Rubio, Roberto, "Lidar Detection of Subvisible Reentry Vehicle Erosive Atmospheric Material," ECOM-5813, March 1977.
50. Low, Richard D.H., and J.D. Horn, "Mesoscale Determination of Cloud-Top Height: Problems and Solutions," ECOM-5814, March 1977.
51. Duncan, Louis D., and Mary Ann Seagraves, "Evaluation of the NOAA-4 VTPR Thermal Winds for Nuclear Fallout Predictions," ECOM-5815, March 1977.
52. Randhawa, Jagir S., M. Izquierdo, Carlos McDonald and Zvi Salpeter, "Stratospheric Ozone Density as Measured by a Chemiluminescent Sensor During the Stratcom VI-A Flight," ECOM-5816, April 1977.
53. Rubio, Roberto, and Mike Izquierdo, "Measurements of Net Atmospheric Irradiance in the 0.7- to 2.8-Micrometer Infrared Region," ECOM-5817, May 1977.
54. Ballard, Harold N., Jose M. Serna, and Frank P. Hudson Consultant for Chemical Kinetics, "Calculation of Selected Atmospheric Composition Parameters for the Mid-Latitude, September Stratosphere," ECOM-5818, May 1977.
55. Mitchell, J.D., R.S. Sagar, and R.O. Olsen, "Positive Ions in the Middle Atmosphere During Sunrise Conditions," ECOM-5819, May 1977.
56. White, Kenneth O., Wendell R. Watkins, Stuart A. Schleusener, and Ronald L. Johnson, "Solid-State Laser Wavelength Identification Using a Reference Absorber," ECOM-5820, June 1977.
57. Watkins, Wendell R., and Richard G. Dixon, "Automation of Long-Path Absorption Cell Measurements," ECOM-5821, June 1977.
58. Taylor, S.E., J.M. Davis, and J.B. Mason, "Analysis of Observed Soil Skin Moisture Effects on Reflectance," ECOM-5822, June 1977.
59. Duncan, Louis D. and Mary Ann Seagraves, "Fallout Predictions Computed from Satellite Derived Winds," ECOM-5823, June 1977.
60. Snider, D.E., D.G. Murcray, F.H. Murcray, and W.J. Williams, "Investigation of High-Altitude Enhanced Infrared Backround Emissions" (U), SECRET, ECOM-5824, June 1977.
61. Dubbin, Marvin H. and Dennis Hall, "Synchronous Meteorlogical Satellite Direct Readout Ground System Digital Video Electronics," ECOM-5525, June 1977.
62. Miller, W., and B. Engebos, "A Preliminary Analysis of Two Sound Ranging Algorithms," ECOM-5826, July 1977.
63. Kennedy, Bruce W., and James K. Luers, "Ballistic Sphere Techniques for Measuring Atomspheric Parameters," ECOM-5827, July 1977.
64. Duncan, Louis D., "Zenith Angle Variation of Satellite Thermal Sounder Measurements," ECOM-5828, August 1977.
65. Hansen, Frank V., "The Critical Richardson Number," ECOM-5829, September 1977.
66. Ballard, Harold N., and Frank P. Hudson (Compilers), "Stratospheric Composition Balloon-Borne Experiment," ECOM-5830, October 1977.
67. Barr, William C., and Arnold C. Peterson, "Wind Measuring Accuracy Test of Meteorological Systems," ECOM-5831, November 1977.
68. Ethridge, G.A. and F.V. Hansen, "Atmospheric Diffusion: Similarity Theory and Empirical Derivations for Use in Boundary Layer Diffusion Problems," ECOM-5832, November 1977.
69. Low, Richard D.H., "The Internal Cloud Radiation Field and a Technique for Determining Cloud Blackness," ECOM-5833, December 1977.

☆U.S. GOVERNMENT PRINTING OFFICE: 1977 777-093/21